

Functionalized graphene oxide as an electrochemical sensing platform for detection of Bisphenol A

Upama Baruah and Devasish Chowdhury*

Material Nano Chemistry Laboratory, Physical Sciences Division, Institute of Advanced Study in Science and Technology (IASST), Paschim Boragaon, Garchuk, Guwahati 781035, Assam, India.

*Corresponding author

DOI: 10.5185/amlett.2018.2067
www.vbripress.com/aml

Abstract

The present work demonstrates the electrochemical detection of the endocrine disruptor Bisphenol A in solution by three different types of functionalized graphene samples viz. graphene oxide (GO), ester functionalized graphene oxide (GO-ES) and amine functionalized graphene oxide (GO-en) modified glassy carbon electrode (GCE) using a very simple drop casting method without the use of any toxic organic compounds or polymeric binders via cyclic voltammetry. The system developed showed detection of BPA via formation of a π -stacked layered functionalized graphene oxide-BPA (π -s-GO-BPA) nanocomposite accompanied by a reduction in the oxidation peak current value associated with a significant shift in the peak potential value. The electrochemical sensing materials developed showed good sensitivity compared to already reported systems and furthermore high selectivity in presence of other structurally similar kinds of molecules in solution without the use of any toxic organic chemicals thereby demonstrating the practical applicability of the material and the technique developed. The practical viability of the material developed is also demonstrated via testing with a real low quality plastic sample that contains Bisphenol A. A plausible mechanism to justify the detection process is also being discussed. Copyright © 2018 VBRI Press.

Keywords: Graphene oxide, functionalization, π - π stacking interaction, cyclic voltammetry, electrochemical detection.

Introduction

Bisphenol A, chemically known as (2,2-bis(4-hydroxyphenyl) propane) is an important industrial chemical owing to its popular uses in widespread fields such as an additive in the manufacture of polycarbonate plastics, epoxy resins, as dental sealants, in water bottles and baby feeding bottles etc. to name a few [1]. This molecule has recently raised much concern among the scientific community which is ascribable to its potential toxic implications in human, animal and aquatic life and also in issues pertaining to the environment.[2,3] Due to the extensive use of this chemical in consumer products, high levels of BPA are regularly being leached into the environment which is commonly caused by incomplete reaction on exposure to heat or acidic and basic conditions accelerating the hydrolysis of the ester bonds linking BPA monomers[4] from plastic food packaging into water or food,[5] with greatest concentrations expected in surface and industrial waste water[6]. BPA is also being listed as an Endocrine Disrupting Chemical (EDC) as it is known to imitate the biological activity of naturally occurring hormones like estrogen [7] with higher concentrations in the blood stream causing reproductive dysfunction, endometrial hyperplasia,

recurrent miscarriages, abnormal karyotypes, and polycystic ovarian syndrome, etc. in both man and animals [8] along with increasing the risk of cancer [9]. Further, leaching of Bisphenol A from baby feeding bottles have led to negative health effects in infants. Owing to the negative effects of Bisphenol A, it has posed recent concern among the scientific community to design and develop easy, clean, cost-effective, selective and sensitive materials and methods for easy detection of this hazardous pollutant. [10]

Conventional methods for detection of Bisphenol A involve chromatographic techniques such as Gas Chromatography or HPLC [11] coupled with Mass Spectroscopy or capillary electrophoresis, solid-phase micro extraction, etc. [2,12,13]. These analytical methods suffer from the drawbacks of being expensive and needs complicated sample pretreatment in addition to not being suitable for on-site operation [14]. Therefore, search for easy and effective ways which are fast and allow easy detection of BPA at a lower cost with high sensitivity is in great demand. In this regard electrochemical techniques can prove to be a useful alternative to the existing traditional methods. It has a host of advantages including rapid response, low energy consumption, on-site applicability, clean and as a eco-

friendly method. [1,15,16] The detection of BPA via electrochemical methods using different modifications of the glassy carbon electrode has already been reported in the literature. For instance, Apodaca et al. investigated electrochemical sensing of BPA via electrochemical impedance spectroscopy (EIS) measurements using an electro polymerized molecularly imprinted polymer film composed of varying ratios of BPA to terthiophene and carbazole monomer complex deposited onto indium tin oxide (ITO) substrates via anodic electro polymerization using cyclic voltammetry (CV)[6]. Li *et al.* reported carboxylate multi-walled nanotube modified GCE for BPA detection [17]. Ndlovu et al. demonstrated a cost-effective bare exfoliated graphite electrode for electrochemical detection of BPA [5].

Graphene, a zero band-gap semiconductor material comprising of a two-dimensional hexagonal honeycomb network of sp^2 hybridized carbon atoms and often termed as a 'wonder material' has been in limelight recently on account of its interesting properties like high conductivity, good biocompatibility, high absorptivity, [18] electronic property, and potential applications in electrochemical sensors [19-21]. Furthermore, due to high electron transport mobility graphene can act as electron transfer bridges making them suitable for electro catalytic applications [22]. On the other hand, graphene functionalized with different surface functional moieties, make them useful non-toxic materials with a large surface area thereby facilitating adsorption of biomolecules which is favorable for designing sensors with improved sensitivity. Also graphene is free from catalytic impurities such as Fe, Ni etc. present in carbon nanotubes thereby limiting the probable interference caused by these metals and hence improving the reproducibility of results [23].

In the present work, we demonstrate the electrochemical detection of Bisphenol A in solution by three different types of functionalized graphene viz. graphene oxide (GO), ester functionalized graphene oxide (GO-ES) and amine functionalized graphene oxide (GO-en) modified glassy carbon electrode (GCE) via formation of π -s-GO-BPA nanocomposite on the electrode surface using a very simple drop casting method without the use of any toxic organic compounds or polymeric binders. The system developed showed detection of BPA via a reduction in the oxidation peak current value associated with a significant shift in the peak potential value. There have been numerous reports available for detection of BPA in solution using various analytical techniques ranging from electrochemical to spectroscopic and so on. On the other hand, the materials reported so far range from graphene, CNT, to various polymers employing different metals and metal oxides like Pt, Au, SiO_2 , Al_2O_3 etc. employing the use of certain toxic organic and inorganic compounds such as azobenzene and its derivatives, thiophenes, carbazoles, silanes etc. Whereas, the system we report herein is based purely on graphene derivatized with different surface functional groups based purely on simple cast and dry strategy under ambient conditions without the

use of any toxic organic compounds or polymeric binders. Further, the electrochemical sensing materials developed showed good sensitivity compared to already reported systems and furthermore high selectivity in presence of other structurally similar kinds of molecules in solution thereby demonstrating the practical applicability of the material and the technique developed. However, the detection mechanism is not proposed to be based on the oxidation of BPA at the electrode which is contrary to earlier reported systems for electrochemical detection of BPA. Also the practical applicability of the functionalized graphene material developed has been demonstrated for detection of Bisphenol A in a real sample i.e. an extract obtained from commercially available plastic cups used for consumption of tea/coffee etc. Thus, the present study is a different approach for electrochemical detection of Bisphenol A as it deals with detection via π -s-GO-BPA nanocomposite formation contrary to conventional methods which deals with oxidation of BPA. A plausible mechanism to justify the detection process is also being discussed.

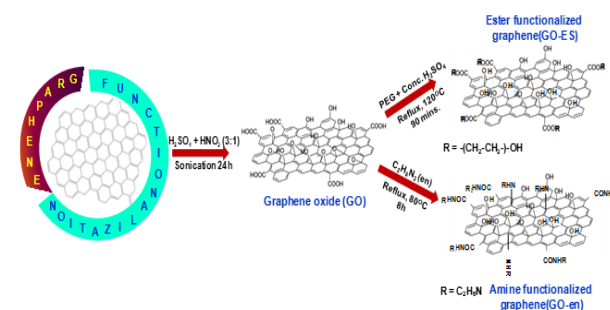
Experimental

Materials and methods

Commercially available graphene platelet Nano powder (GPN Type 1, thickness 6–8 nm) was purchased from Sisco Research Laboratories Pvt. Ltd., ethylene diamine ($\geq 98\%$), concentrated sulfuric acid H_2SO_4 , concentrated nitric acid HNO_3 , 4-nitrotoluene, m-nitrophenol, 1-amino-2-naphthol-4-sulphonic acid, potassium ferricyanide $K_3[Fe(CN)_6]$ and potassium chloride KCl were purchased from Merck Specialties Pvt. Ltd., Poly (ethylene glycol) and 2,2'-dithiobenzoic acid was purchased from Sigma Aldrich. All chemicals were used as received without further purification. The water used throughout the experiments was from a Milli-Q water purification system.

Synthesis of graphene with different surface functionalities

Functionalized graphene samples were prepared using different chemical reactions to incorporate various surface functionalities on to the graphene surface. The pictorial representation of the reaction processes is being demonstrated in **Scheme 1**.



Scheme 1. Schematic representation of the synthesis of functionalized graphene samples using various chemical reaction.

Synthesis of graphene oxide (GO) with carboxylic acid (-COOH), hydroxyl (-OH) and epoxy (-O-) surface functional groups

Graphene platelet Nano powder was exfoliated and oxidized in a one-step process employing an acid mixture oxidant i.e., a 3:1 mixture of concentrated H₂SO₄/HNO₃ using a simple bath sonication and centrifugation technique at room temperature [24]. The reactive species of the process responsible for the oxidation is nitronium ion (NO₂⁺) [25].



Briefly, a 50 mL dispersion of graphene platelet Nano powder was prepared by dispersing 0.01 g of graphene platelet Nano powder in a 3:1 acid mixture of concentrated H₂SO₄ (98 wt%): HNO₃ (70%). This dispersion was then subjected to bath sonication for a time period of 24 hours in a water bath. After sonication the dispersion was diluted by adding 100 mL of deionized water and centrifuged at 8000 rpm for 30 minutes to separate the exfoliated graphene from the acid mixture. The supernatant solution containing the acid mixture was then separated from the heavier particles and this process of centrifugation and washing was repeated until all the acid content was washed away. Finally, the exfoliated graphene part was redispersed in deionized water and this dispersion was termed as the graphene oxide (GO) solution.

Synthesis of ester functionalized graphene oxide (GO-ES) with ester (-COOR) and hydroxyl (-OH) surface functional groups

Graphene oxide (GO) prepared from the above step was then subsequently functionalized via incorporation of ester (-COOR) functional groups using covalent bonding interactions according to a method previously reported by our laboratory [26].

In a typical procedure, the aqueous dispersion of GO was mixed with poly (ethylene glycol) (PEG) in a 1:2 ratios (5 mL GO dispersion + 10 mL PEG), and to this mixture, approximately 40 μL of concentrated sulphuric acid was added as the catalyst. The solution was subsequently heated at 120°C under reflux for 90 minutes with continuous stirring. The resultant dispersion obtained was the esterified GO solution, termed as GO-ES. In this case, the fruity smell of the product was used as a preliminary indication of the formation of ester-functionalized GO.

Synthesis of amine/amide functionalized graphene oxide (GO-en) with amine (-NHR), amide (-CONHR) and hydroxyl (-OH) surface functional groups

Graphene oxide sample prepared was reduced and functionalized in a single step via incorporation of amine and amide functionalities on the surface using ethylene diamine (en) in accordance with our previous reports [27]. For the reduction and functionalization typically

10 mL of the as-prepared GO dispersion was taken in a round bottom flask and to it 15 mL of 33% ethylene diamine solution was added dropwise with continuous stirring. The pH of the reaction mixture was adjusted at around 10 and the dispersion was refluxed for 8 hours at 80°C. The mechanism of reduction and functionalization of GO by ethylene diamine via ring opening of epoxy groups has already been reported earlier by us and other groups [27,28]. The proposed mechanism for the reduction of GO by ethylene diamine occurs via reaction of diamine with epoxy groups by a ring opening addition reaction; the driving force for the reaction being the strain on the three-membered epoxy ring which always has a tendency to open up. Further some of the amine groups will also react with the carboxylic acid groups on the GO surface to form covalent amide linkages thereby leading to covalent functionalization. The GO dispersion reduced and functionalized with ethylene diamine was termed as GO-en.

Preparation of functionalized graphene-modified glassy carbon electrode (GCE)

The functionalized graphene modified GCE was prepared by a simple drop casting method. Firstly, the surface of GCE was mechanically polished using alumina powder of diameter 0.05 μm and rinsed ultrasonically with Milli-Q water and ethanol respectively. The electrode was then completely dried at room temperature prior to use. Approximately 1mg of graphene oxide, ester functionalized graphene oxide and amine functionalized graphene oxide were dispersed in 1 mL of distilled water and ultra-sonicated for 30 minutes for proper dispersibility. About 5 μL of the respective functionalized graphene dispersions was then cast on the surface of GCE and dried at 60°C in a hot air oven to form a uniform film on the surface.

Electrochemical detection of Bisphenol A (BPA) by the functionalized graphene modified GCE

Cyclic voltammetry (CV) was performed to demonstrate the electrochemical sensing of BPA by the functionalized graphene modified GCE. All measurements were done using 10 mL of a 1:1 mixture of 2mM potassium ferricyanide K₃[Fe(CN)₆] and 0.1 M potassium chloride KCl as the supporting electrolyte. The operating potential ranges were found to be different for different functionalized graphene-modified electrodes. In all cases the cyclic voltammograms were recorded at a scan rate of 0.05 mV/s. The three-electrode system viz. the working electrode (the functionalized graphene modified GCE, surface area of electrode = 28.27 mm², diameter 6 mm), the reference electrode (Ag/AgCl) and the counter electrode (Pt wire) dipped in the electrolyte solution and all connections were made accordingly. A specific amount of the analyte i.e. Bisphenol A solution in ethanol was added to the electrolyte mixture at regular intervals and the corresponding CV graph was recorded.

Characterization

UV-visible absorption spectra of the prepared samples were collected on a Shimadzu UV-VIS Spectrophotometer, UV-2600; zeta potential measurements were carried out on a Malvern Zetasizer Nano series, Nano-ZS90. Scanning Electron Microscope (SEM) images were collected on a Carl Zeiss Sigma VP instrument. Powder X-ray diffraction (XRD) spectrum was collected on a Bruker D8 Advance diffractometer. The presence of different functionalities on the prepared samples was confirmed using Fourier Transform Infrared Spectra collected on a Nicolet-6700 FT-IR Spectrophotometer. Cyclic Voltammetry (CV) experiments for electrochemical detection of Bisphenol A were performed on a CH instrument Electrochemical Workstation using the conventional three-electrode system viz. a platinum wire auxiliary electrode, an Ag/AgCl electrode as the reference electrode and the bare or functionalized graphene modified glassy carbon electrode (GCE).

Results and discussion

Physical characterization of the functionalized graphene samples prepared

The functionalized graphene samples prepared were characterized in a stepwise and systematic manner using UV-Visible absorption spectroscopy, zeta potential measurements, Scanning Electron Microscopy, Powder XRD and Fourier Transform Infrared (FT-IR) Spectroscopy.

UV-visible spectroscopy

Graphene oxide (GO), ester functionalized graphene oxide (GO-ES) and amine/amide functionalized graphene oxide (GO-en) samples were characterized using UV-Visible spectroscopy. The corresponding stacked UV-Visible absorption spectra of the samples are shown in Fig. 1.

The UV-Visible absorption spectrum of Graphene oxide (GO) shows two distinct absorption peaks viz. at 201 nm and 280 nm which can be ascribed respectively to $\pi-\pi^*$ transition of the C=C bond and to $n-\pi^*$ transition of the $-\text{COO}^-$ groups arising due to oxidation of graphene. The presence of these characteristic absorption peaks indicates the successful oxidation of graphene nano platelets to graphene oxide. On the other hand, the ester functionalized graphene (GO-ES) shows an absorption peak at 272 nm corresponding to $n-\pi^*$ transition of the ester ($-\text{COOR}$) group. This indicates the successful incorporation of ester functional groups into the graphene surface.

Further, after reduction cum functionalization of graphene oxide with ethylene diamine, the absorption peak of GO corresponding to $n-\pi^*$ transition of the $-\text{COO}^-$ groups arising due to oxidation of graphene was found to disappear indicating a successful reduction of $-\text{COOH}$ groups with a steep increase in absorption around 200 nm. This increase may however be ascribed to $n-\sigma^*$

transitions of the $-\text{OH}$ and $-\text{NH}_2$ groups on the surface of GO-en. Therefore, UV-Visible spectroscopy provides convincing evidence supporting the successful incorporation of different functional groups on to the graphene surface.

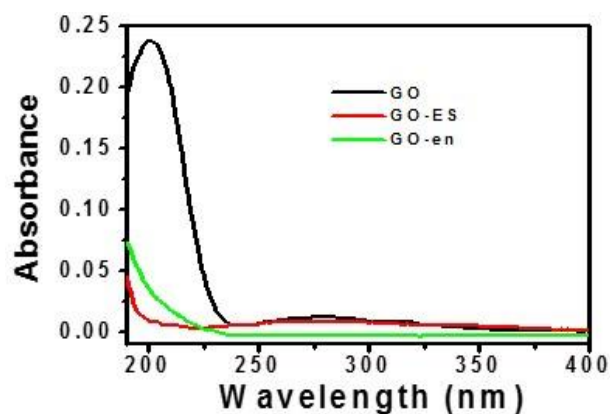


Fig. 1. UV-visible absorption spectra of Graphene oxide (GO), ester functionalized graphene oxide (GO-ES) and amine/amide functionalized graphene oxide (GO-en) samples showing the characteristic electronic transitions.

Scanning Electron Microscopy and Zeta potential measurements

Evidence for successful synthesis of the functionalized graphene samples could be drawn from Scanning Electron Microscopy and Zeta Potential Measurements. SEM samples were prepared by drop casting a dilute solution of functionalized graphene samples on silicon wafer substrates. Fig. 2 (A)-(C) shows the SEM micrographs of GO, GO-ES and GO-en respectively.

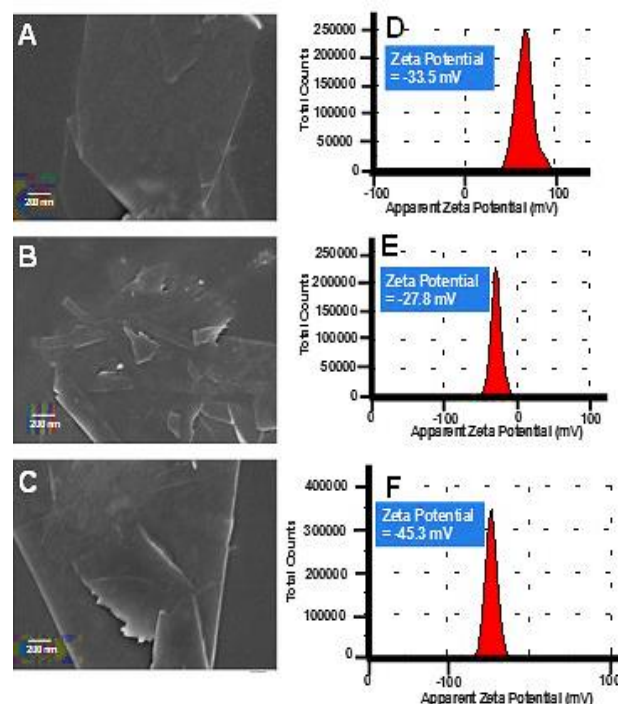


Fig. 2. SEM micrographs (A)-(C) and (D)-(F) zeta potential distribution graphs of GO, GO-ES and GO-en respectively.

All the images show the planar sheet-like structure of the exfoliated graphene functionalized with different surface functional groups. Zeta potential analysis was done using a dilute colloidal solution of the functionalized graphene samples dispersed in water i.e. at neutral pH. **Fig. 2 (D)-(F)** shows the zeta potential distribution graphs of the samples GO, GO-ES and GO-en respectively. GO was found to exhibit a zeta potential value of -33.5 mV thereby showing the negative potential on the surface of GO. After esterification of GO to GO-ES, the value of zeta potential was found to be reduced to -27.8 mV indicating a positive change in the surface charge from more negative to less negative upon esterification.

This observation is quite justifiable based on the fact that the $-\text{COOH}$ group bearing GO becomes less negative after esterification to form $-\text{COOR}$ ($R =$ alkyl chain) [26]. On the other hand, reduction cum amination of GO using ethylene diamine causes an increase in the zeta potential value of GO from -33.5 mV to -45.3 mV. This observation can be ascribed to the increased electron density upon formation of $-\text{OH}$ groups via ring opening of epoxy groups and formation of $-\text{NHCH}_2-\text{CH}_2-\text{NH}_2$ linkages. Further, upon reduction with en, the $\text{C}=\text{C}$ structure was somewhat restored leading to an increase in the overall negative charge. Therefore, zeta potential measurements provide strong and convincing evidence supporting the successful functionalization of graphene samples bearing different surface functionalities.

FT-IR and powder XRD analysis

All the three samples of functionalized graphene prepared were characterized by FTIR spectroscopy for inquiring the successful incorporation of the respective functional groups using KBr as the reference standard.

Fig. 3 (A) shows the stacked FTIR spectra of GO, GO-ES and GO-en. The stretching frequencies observed for GO appear at 3483 ($-\text{O}-\text{H}$ stretch), 2961 ($-\text{C}-\text{H}$ stretch), 1708 ($\text{C}=\text{O}$ carboxylic acids), 1384 , 1159 ($\text{C}-\text{O}$ stretch alcohols), 1081 ($=\text{C}-\text{H}$ bend) and 883 ($\text{O}-\text{H}$ bend carboxylic acid). GO-ES showed the characteristic peaks at 3401 ($-\text{O}-\text{H}$ stretch), 2881 ($\text{C}-\text{H}$ stretch alkanes), 1642 ($\text{C}=\text{O}$ ester) [26], 1458 ($\text{C}-\text{H}$ bend alkanes), 1352 ($\text{C}-\text{O}$ stretch alcohols) and 1118 ($=\text{C}-\text{H}$ bend). The stretching frequencies for GO-en were found to appear at 3400 ($-\text{O}-\text{H}$ stretch), 2984 ($-\text{C}-\text{H}$ stretch), 1587 ($\text{N}-\text{H}$ bend 1° amines) [27], 1385 ($\text{C}-\text{O}$ stretch alcohols), 1050 ($\text{C}-\text{O}$ stretch alcohols) and 811 ($\text{C}-\text{H}$ rock). Thus from FTIR spectroscopy it can be very well established that the graphene samples have been successfully functionalized by different functional moieties.

The functionalized graphene samples prepared were also subjected to powder X-ray diffraction analysis and the corresponding stacked diffractograms are shown in **Fig. 3 (B)**. It is very clear from the graph that the diffractograms for all the functionalized graphene samples viz. GO, GO-ES and GO-en show a very sharp and well-defined diffraction peak at $2\theta \approx 25^\circ$ (002)

corresponding to the disorderly stacked graphene sheets. Further, the sharpness of the peaks observed clearly indicate the crystalline nature of the graphene samples.

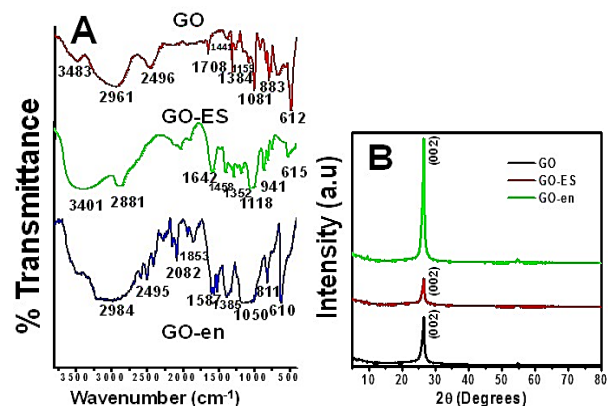


Fig. 3. Stacked (A) FT-IR spectra and (B) Powder XRD spectra of functionalized graphene samples prepared viz. GO, GO-ES and GO-en.

Electrochemical characterization of functionalized graphene modified glassy carbon electrode

The electrochemical behavior of functionalized graphene modified glassy carbon electrode was investigated using potassium ferricyanide as the redox marker via cyclic voltammetry (CV) measurements. All measurements were carried out using 10 mL of a $1:1$ mixture of 2 mM potassium ferricyanide $\text{K}_3[\text{Fe}(\text{CN})_6]$ and 0.1 M potassium chloride KCl as the supporting electrolyte. The operating potential ranges were found to be different for different functionalized graphene-modified electrodes. In all cases, the cyclic voltammograms were recorded at a scan rate of 0.05 mV/s. **Fig. 4** shows the stacked cyclic voltammograms of bare and different functionalized graphene modified GCE.

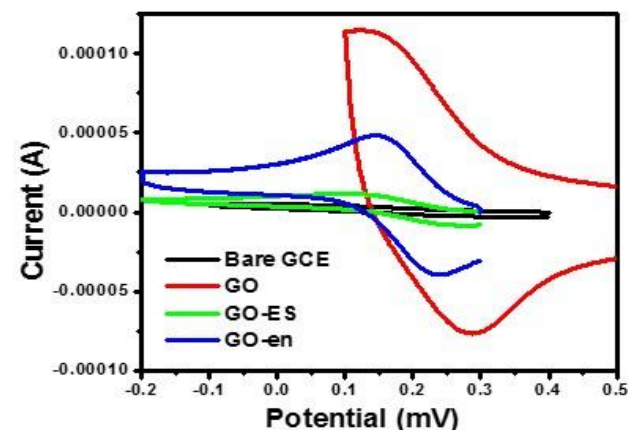


Fig. 4. Stacked cyclic voltammograms of bare and different functionalized graphene (oxidized, esterified and amine reduced graphene) modified GCE.

From the plot it is quite clear that all of the functionalized graphene samples exhibit a well-defined oxidation/reduction peak when compared to the bare

GCE in the potential window of -0.2 - 0.6 V. The CV graph of GO shows a well-defined oxidation peak at about 0.28 V. From the plot it is very clear that the electron transfer process is an irreversible one. On the other hand, the voltammogram of esterified graphene i.e., GO-ES shows a well-defined reduction peak at a potential value of 0.109 V. In this case too, the electron transfer was found to be an irreversible one although in the reverse order as compared with that of GO. For ethylene diamine reduced and functionalized graphene, i.e., GO-en, two distinct oxidation-reduction peaks were found to appear at 0.24 V and 0.15 V respectively giving rise to an approximately symmetrical CV graph thereby indicating a reversible electron transfer process. It is to be noted here that in all the cases the oxidation/reduction peak currents were found to be higher than that of the bare GCE indicating that the prepared graphene samples were successfully deposited on the surface of GCE and thereby exhibit higher conductivity as compared to the bare GCE.

Electrochemical detection of Bisphenol A by the functionalized graphene modified glassy carbon electrode

After careful investigation of the electrochemical response of different functionalized graphene modified GCE, we next carried out the CV experiments in a similar manner in presence of the environmentally hazardous analyte Bisphenol A. All measurements were carried out as before using 10 mL of a $1:1$ mixture of 2 mM potassium ferricyanide $K_3[Fe(CN)_6]$ and 0.1 M potassium chloride KCl as the supporting electrolyte. Different concentrations of the analyte i.e. Bisphenol A solution in ethanol was added to the electrolyte mixture at regular intervals and the corresponding CV graph was

recorded at a scan rate of 0.05 mV/s. **Fig. 5** shows the electrochemical response of various functionalized graphene modified GCE both in the presence and absence of Bisphenol A in solution. **Fig. 5 (A)** shows the stacked cyclic voltammograms of GO-modified GCE in both the presence and absence of BPA (i.e. both before and after formation of π -s-GO-BPA nanocomposite) on the electrode surface. The CV graph of GO shows a well-defined oxidation peak at about 0.28 V.

From the plot it is very clear that the electron transfer process for GO-GCE is an irreversible one. However, after formation of π -s-GO-BPA nanocomposite on the GCE surface, the oxidation peak current was found to be reduced as evident from the CV graph of GO-GCE in presence of BPA. The complete profile showing the electrochemical response of GO towards Bisphenol A in the concentration range $1.99 \times 10^{-7} - 11.15 \times 10^{-8}$ M is shown in **Fig. S1 (A)** (Supplementary Information, SI). **Fig. 5 (D)** shows the calibration curve of the oxidation peak current against various concentrations of BPA added. From the plot it is evident that the reduction in the oxidation current shows a good linear response with a linear regression constant value of $R^2 = 0.8202$. It is to be mentioned that all data were averaged over a set of three consecutive experiments and the calibration curves show the corresponding error bars demonstrating good reproducibility of the results obtained. **Fig. 5(B)** shows the stacked cyclic voltammograms of GO-modified GCE in both the presence and absence of BPA (i.e. both before and after formation of π -s-GO-ES-BPA nanocomposite) on the electrode surface. The voltammogram of esterified graphene modified GCE i.e., GO-ES-GCE shows a well-defined reduction peak at a potential value of 0.109 V. In this case the reduction peak current was found to appear at a potential value of -0.044 V π -s-GO-

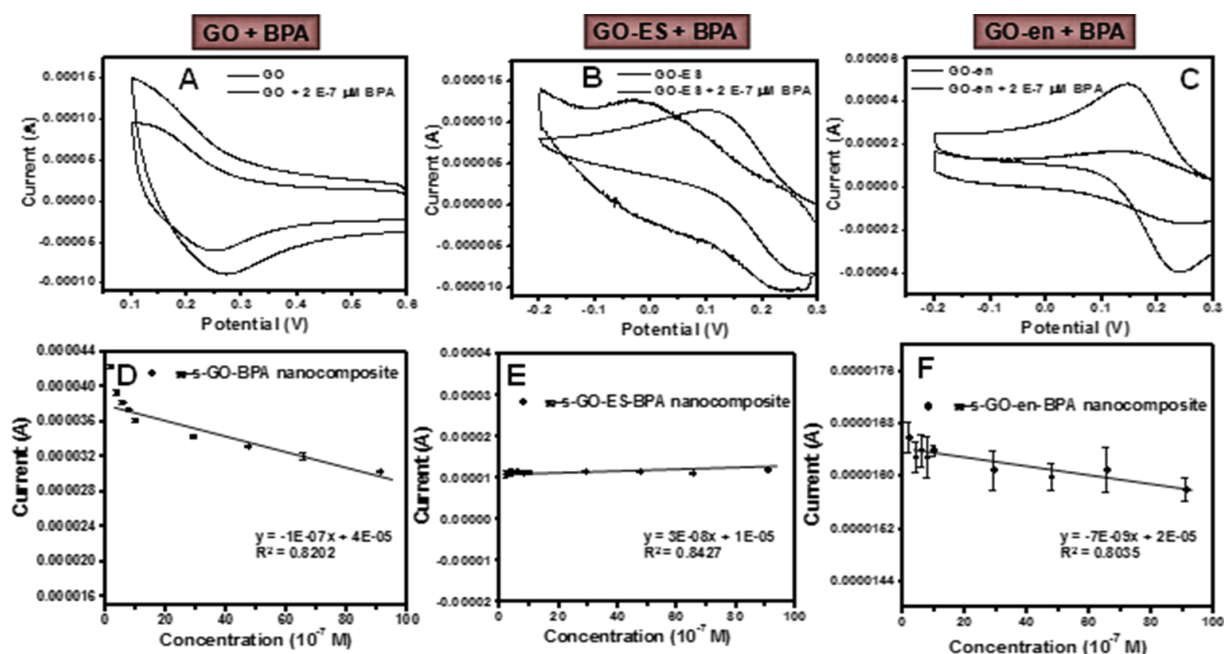


Fig. 5. Stacked CV graphs showing the electrochemical response towards the presence of Bisphenol A for (A) GO, (B) GO-ES and (C) GO-en modified GCE. Calibration curves (Current vs. Concentration of BPA) showing the linear response of (D) GO, (E) GO-ES and (F) GO-en modified GCE towards the presence of Bisphenol A in solution.

ES-BPA nanocomposite on the electrode surface with an increase in the value of reduction peak current and a marked shift in the peak maxima of 0.065 V. The complete profile showing the electrochemical response of GO-ES towards Bisphenol A in the concentration range $1.99 \times 10^{-7} - 11.15 \times 10^{-8}$ M is shown in **Fig. S1 (B)**, SI. **Fig. 5 (E)** shows the calibration curve of the oxidation peak current against various concentrations of BPA added for GO-ES-GCE. From the plot it is evident that the reduction in the oxidation current shows a good linear response with a linear regression constant value of $R^2 = 0.8427$. Similarly, for ethylene diamine reduced and functionalized graphene modified GCE, i.e., GO-en-GCE, two distinct oxidation-reduction peaks were found to appear at 0.24 V and 0.15 V respectively. In this case too there was an observed decrease in the oxidation/reduction peak currents in the presence of BPA as the analyte i.e. upon formation of π -s-GO-en-BPA nanocomposite on the electrode surface as evident from **Fig 5(C)**. The complete profile showing the electrochemical response of GO-en towards Bisphenol A in the concentration range 1.99×10^{-7} - 11.15×10^{-8} M is shown in **Fig S1 (C)**, SI. **Fig 5 (F)** shows the calibration curve of the oxidation peak current against various concentrations of BPA added for GO-en-GCE. From the plot it is evident that the decrease in the oxidation/reduction current values shows a good linear response with a linear regression constant value of $R^2 = 0.8035$. Thus from the plots it is quite evident that in all of the functionalized graphene modified GCEs there was an observed change in the redox behavior of the native material (i.e., functionalized graphene) in presence of Bisphenol A due to gradual formation of the π -stacked functionalized GO-modified GCE surface.

Analysis of real sample

The potential applicability of any material developed as a sensor is not fully understood unless it is practically viable. Hence to demonstrate the practical viability of the material developed, we carried out the electrochemical sensing experiment for a real sample.

As Bisphenol A is a major additive used in the manufacture of plastic articles of day to day use like plastic bottles etc., we decided to check the leaching out of the compound from commercially available plastic cups used extensively for consumption of tea/coffee etc. The detailed procedure followed for preparation of the extract from the plastic cups is described in the Supporting Information. Cyclic voltammetry experiment was carried out in a similar manner as for the pure sample (Bisphenol A). However, in this case the extract was added in successive amounts to the electrolyte and the voltammograms were recorded using the GO-modified GCE. The corresponding stacked CV graphs upon successive addition of the plastic extract are shown in **Fig 6**. As evident from the graph, there was an observed decrease in the oxidation peak current upon successive addition of the plastic extract. This response was found to be similar to that obtained upon addition of Bisphenol A in the pure state as demonstrated earlier.

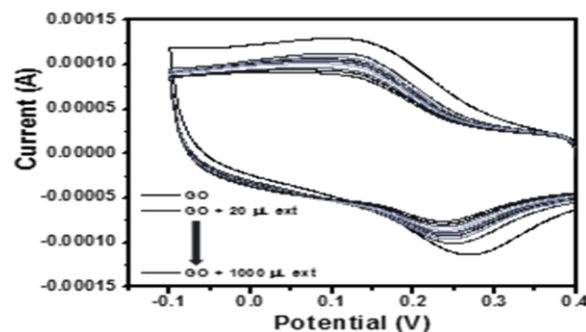


Fig. 6. The stacked cyclic voltammograms of GO-modified GCE in the presence of extract obtained from plastic cups.

As the electrochemical response of the GO modified GCE towards the plastic extract was found to be convincing and in close proximity to results obtained with the pure compound, we next decided to confirm whether the extract obtained from the plastic cups actually contained Bisphenol A leached out during preparation of extract. For this we carried out LCMS analysis of both the pure compound (Bisphenol A) as the standard and the extract obtained from plastic cups as the sample.

Fig. 7 shows the LCMS spectra of both the pure Bisphenol A and the extract. From the mass spectra it is quite clear that the extract obtained from plastic cups contained a significant amount of Bisphenol A as observed from the position of the major peak at the exactly same m/z value of 227.11 as that of pure Bisphenol A. This confirms the leaching out of Bisphenol A from the plastic cups into the extract with limits detectable by the GO modified GCE via cyclic voltammetry. Thus this analysis confirms the practical applicability of the GO-modified GCE for electrochemical detection of Bisphenol A.

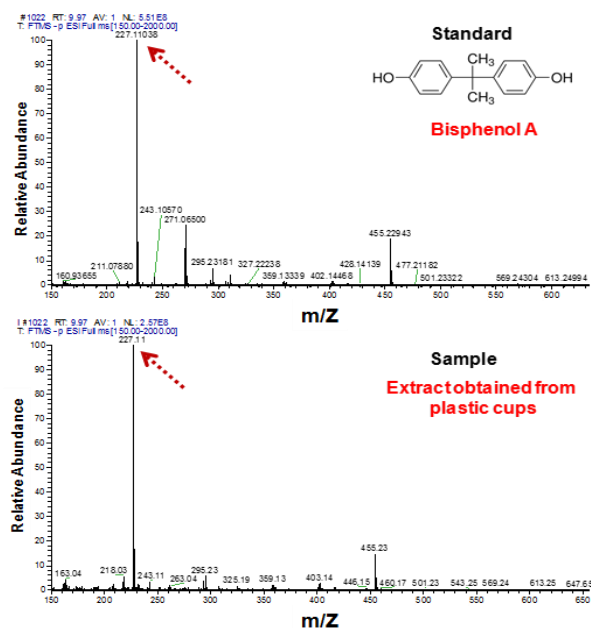


Fig. 7. The mass spectra of Bisphenol A both in the pure state and in the extract obtained from plastic cups clearly showing the presence of Bisphenol A in the extract.

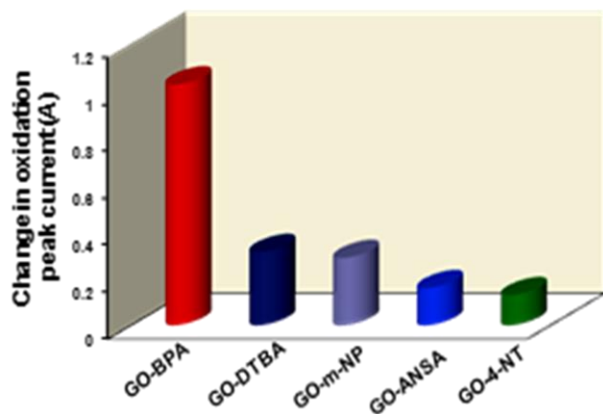


Fig. 8. Histogram plot of the change in oxidation peak current of GO-modified GCE in the presence of various types of analytes bearing a variety of functional groups.

Selectivity of the functionalized graphene based electrode material developed towards electrochemical detection of Bisphenol A

For a material to be applicable as a sensor it must exhibit good selectivity towards the detection of the specific analyte concerned. Therefore, keeping this point in view, we carried out the electrochemical sensing of a few other analytes structurally similar to BPA viz. 2,2'-dithiobenzoic acid (DTBA), 4-nitrotoluene (4-NT), m-nitrophenol (m-NP) and 1-amino-2-naphthol-4-sulphonic acid (ANSA) using GO-modified GCE. **Fig. 8** shows the histogram plot of the change in oxidation peak current of GO-modified GCE in the presence of various types of analytes bearing a variety of functional groups.

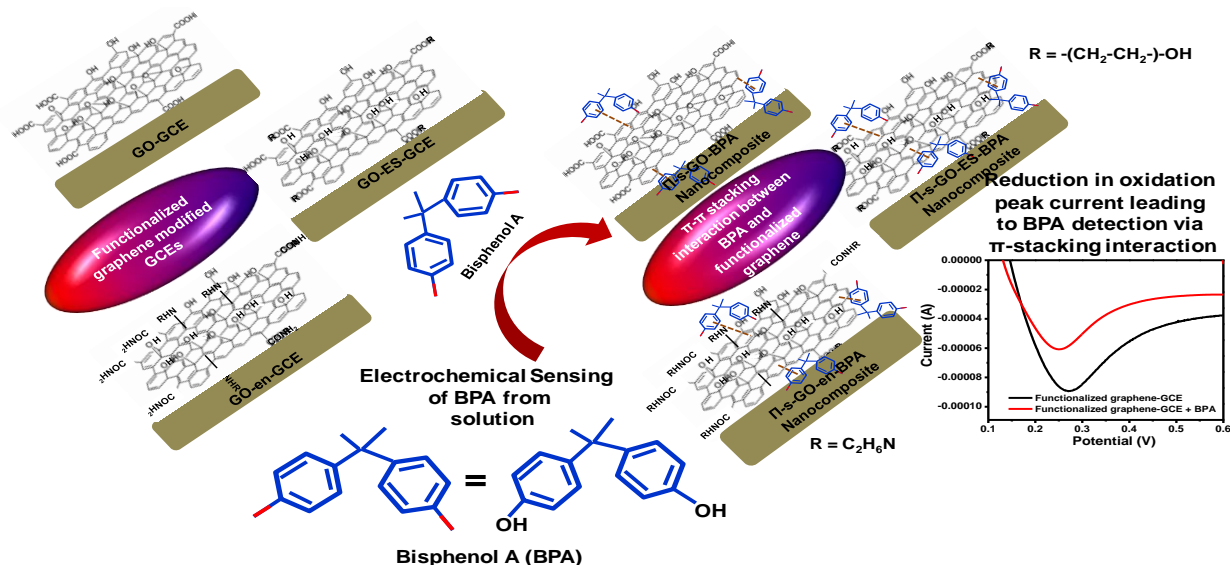
All experiments were performed under exactly same conditions as was done for BPA. The concentration of the analytes used was 1.99×10^{-7} M similar to the lowest detectable amount of BPA by the functionalized

graphene modified GCE. It is quite clear from the plot that the change in current is highest in presence of BPA as compared to all other analytes in solution. The stacked cyclic voltammograms of GO modified GCE both in the presence and absence of different analytes is shown in **Fig. S2** (A-D), SI. Therefore, we can say that GO-modified GCE can be potentially used for the selective detection of Bisphenol A in solution in presence of other similar types of molecules.

Mechanistic insight

As evident from the cyclic voltammograms of different functionalized graphene modified GCEs in presence of BPA, there is an observed decrease in the oxidation peak current of the native graphene materials along with a significant shift in the oxidation peak potential. Although most of the earlier reports on electrochemical detection of BPA by modified GCEs are based primarily on the oxidation of BPA, [14,29-31] the system we report herein do not claim the oxidation of BPA at the electrode. Rather it can probably be demonstrated as a simple detection of BPA in solution with the detection process being driven by the π - π attraction between the functionalized graphene modified surface of the GCE and the BPA molecules in solution as demonstrated in **Scheme 2** forming a π -stacked nanocomposite layer on the GCE surface.

Further, it is to be noted that the π -stacking of BPA molecules on the graphene modified GCE does not lead to an increase in the oxidation current and rather shows a decrease which is contrary to available literature reports. [32] This contrasting observation can be attributed to the fact that the functionalized graphene material used viz. GO, GO-ES or GO-en is composed primarily of a sp^3 C-framework with small sp^2 domains in the sheet structure. π -stacking of BPA molecules occur specifically at those domains and these sp^2 regions being discrete, the resulting current increase is not



observed. However, they serve as the driving force to draw the BPA molecules to the electrode surface via π -stacking interaction as evident from the reduced oxidation peak current of the graphene samples along with a marked shift in the oxidation potential from more to less negative side thereby leading to electrochemical detection of BPA in solution by the functionalized graphene modified GCEs.

Comparative Analysis of the sensitivity of the electrodes developed towards detection of Bisphenol A: A review of literature

For comparative analysis of the materials we developed viz. GO, GO-ES and GO-en for preparation of functionalized graphene-modified GCE for electrochemical detection of Bisphenol A, we present herein a summary of different systems already reported for detection of BPA using various analytical techniques. **Table 1** lists the different types of materials and analytical techniques already reported for detection of Bisphenol A along with the corresponding detection limits based on literature review.

From the table it is quite clear that there are already a number of reports available for detection of BPA in solution using various analytical techniques ranging from electrochemical to spectroscopic and so on. On the other hand, the materials reported range from graphene, CNT, to various polymers employing different metals and metal oxides like Pt, Au, SiO₂, Al₂O₃ etc. At the same time, it is quite evident that the reported systems made use of certain toxic organic and inorganic compounds such as azobenzene and its derivatives, thiophenes, carbazoles, silanes etc.

On the other hand, the system we report herein is based purely on graphene derivatized with different surface functional groups. Moreover, we carried out the

electrode modification without the use of any polymeric binder, based purely on cast and dry strategy under ambient conditions. Further, the limits of detection reported for the various systems were found to be quite comparable with that obtained with the system we developed in addition to the fact that we did not make use of any toxic organic chemicals or metals in the development of the graphene - based electrode material and that only simple chemical reactions were carried out to incorporate the desired surface functionalities.

Conclusion

In the present study we demonstrated the successful electrochemical detection of the environmentally hazardous endocrine disruptor Bisphenol A using three different chemically functionalized graphene samples viz. GO, GO-ES (ester-functionalized) and GO-en (amine-reduced and functionalized) graphene. All the functionalized graphene samples were subjected to systematic and stepwise characterization using various instrumental techniques. Subsequently, the graphene samples prepared were used to modify the surface of the GCE using a simple drop casting technique under ambient conditions and the corresponding electrode was used for electrochemical sensing of BPA in solution using cyclic voltammetry as a tool. However, the detection mechanism was attributed to simple π -stacking interactions between the sp² domains on the graphene layer structure and the Bisphenol A molecules gradually forming a π -stacked functionalized graphene-BPA nanocomposite on the GCE surface which is in stark contrast to earlier reported sensors which are primarily based on oxidation of Bisphenol A. Therefore, we successfully designed and developed a simple, cost-effective, environmentally benign electrode material based on functionalized graphene for selective and

Table 1. Comparative analysis of the system developed (Functionalized Graphene) with already reported systems available for detection of environmentally hazardous Bisphenol A.

Sl. No.	Material used	Method of detection	Lower detection limit (M)	Reference
1	Graphene-CNTs nanocomposite with a sandwich lamination Structure loaded with Pt nanoparticles	Differential Pulse Voltammetry (DPV)	4.2×10^{-8}	33
2	Surface molecular imprinting polymer microspheres synthesized on silica Microspheres using a water-soluble azobenzene-containing 4-[(4-methacryloyloxy)-phenylazo]benzenesulfonic acid as the functional monomer	UV-Visible spectroscopy	2.19×10^{-6}	34
3	A composite material based on a metal organic framework, nanowhisker of Al ₂ O ₃ silanized with (3-aminopropyl)triethoxysilane and gold nanoparticles.	Differential Pulse Voltammetry (DPV)	3.78×10^{-7}	30
4	An electropolymerized molecularly imprinted polymer (E-MIP) film composed of varying ratios of BPA-terthiophene and carbazole monomer complex deposited onto indium tin oxide (ITO) substrates	Electrochemical Impedance Spectroscopy (EIS)	4.2×10^{-2}	6
5	Graphene-graphene oxide	Cyclic voltammetry & Electrochemical Impedance Spectroscopy (EIS)	4.69×10^{-8}	18
6	Our system	Cyclic voltammetry	1.99×10^{-7}	

sensitive detection of Bisphenol A in solution with a lower detection limit of 1.99×10^{-7} M. Most importantly, we could successfully demonstrate the practical applicability of GO-modified GCE for detection of Bisphenol A leaching out of plastic articles (plastic cups) used frequently for consumption of tea/coffee etc. which can cause major environmental and health hazards. Thus, we believe that we could be successful in designing an eco-friendly material which can provide an easy, cost-effective detection of a major environmental pollutant via an alternative detection mechanism contrary to available reports.

Acknowledgements

This work was supported by SERB, New Delhi, Grant No. SB/S1/PC-69/2012 and BRNS, Mumbai, Grant No. 34/14/20/2014-BRNS. UB wants to thank CSIR, New Delhi for fellowship.

Author's contributions

Authors have no competing financial interests.

Supporting information

Supporting informations are available from VBRI Press.

References

1. Yina, H.; Zhou, Y.; Xu, J.; Ai, S.; Cui, L.; Zhu, L. *Anal. Chim. Acta* **2010**, *659*, 144.
DOI: [10.1016/j.aca.2009.11.051](https://doi.org/10.1016/j.aca.2009.11.051)
2. Alkassir, R. S.; Ganesana, M.; Won, Y. H.; Stanciu, L.; Andreescu, S. *Biosens Bioelectron* **2010**, *26*, 43–49.
DOI: [10.1016/j.bios.2010.05.001](https://doi.org/10.1016/j.bios.2010.05.001)
3. Ballesteros-Gómez, A.; Rubio, S.; Pérez-Bendito, D.; *J Chromatogr A*, **2009**, *1216*, 449–469.
DOI: [10.1016/j.chroma.2008.06.037](https://doi.org/10.1016/j.chroma.2008.06.037)
4. Richter, C. A.; Birnbaum, L. S.; Farabolini, F.; Newbold, R. R.; Rubin, B. S.; Talsness, C. E.; Vandenberg, J. G.; Walsler, D. R.; VomSaal, F. S. *Reprod. Toxicol.* **2007**, *24*, 199–224.
DOI: [10.1016/j.reprotox.2007.06.004](https://doi.org/10.1016/j.reprotox.2007.06.004)
5. Ndlovu, T.; Arotiba, O. A.; Sampath, S.; Krause, R. W.; Mamba, B. B. *Sensors* **2012**, *12*, 11601–11611.
DOI: [10.3390/s120911601](https://doi.org/10.3390/s120911601)
6. Apodaca, D. C.; Permites, R. B.; Ponnappati, R.; Del Mundo, F. R.; Advincula, R. C. *Macromolecules* **2011**, *44*, 6669–6682.
DOI: [10.1021/ma2010525](https://doi.org/10.1021/ma2010525)
7. Yoshida, T.; Horie, M.; Hoshino, Y.; Nakazawa, H. *Food Addit. Contam.* **2001**, *18*, 69–75.
DOI: [10.1080/026520301446412](https://doi.org/10.1080/026520301446412)
8. Cao, X.-L.; Corriveau, J.; Popovic, S. *J. Agric. Food Chem.* **2009**, *57*, 1307–1311.
DOI: [10.1021/jf803213g](https://doi.org/10.1021/jf803213g)
9. Soto, A. M.; Sonnenschein, C. *Nat Rev Endocrinol.* **2010**, *6*, 363–370.
DOI: [10.1038/nrendo.2010.87](https://doi.org/10.1038/nrendo.2010.87)
10. Wu, L.; Deng, D.; Jin, J.; Lu, X.; Chen, J. *Biosens. Bioelectron.* **2012**, *35*, 193–199.
DOI: [10.1016/j.bios.2012.02.045](https://doi.org/10.1016/j.bios.2012.02.045)
11. Liu, X.; Feng, H.; Liu, X.; Wong, D. K. Y. *Anal. Chim. Acta* **2011**, *689*, 212–218.
DOI: [10.1016/j.aca.2011.01.037](https://doi.org/10.1016/j.aca.2011.01.037)
12. Chang, C. M.; Chou, C. C.; Lee, M. R. *Anal. Chim. Acta* **2005**, *539*, 41–47.
DOI: [10.1016/j.aca.2005.03.051](https://doi.org/10.1016/j.aca.2005.03.051)
13. C. Nerin, M. R. Philo, J. Salafranca and L. Castle, *J Chromatogr A*, **2002**, *963*, 375–380.
DOI: [10.1016/S0021-9673\(02\)00554-X](https://doi.org/10.1016/S0021-9673(02)00554-X)
14. Shen, R.; Zhang, W.; Yuan, Y.; He, G.; Chen, H. *J Appl Electrochem* **2015**, *45*, 343–352.
DOI: [10.1007/s10800-015-0792-5](https://doi.org/10.1007/s10800-015-0792-5)
15. Huang, W. *Bull. Korean Chem. Soc.* **2005**, *26*, 1560–1564.
DOI: [10.5012/bkcs.2005.26.10.1560](https://doi.org/10.5012/bkcs.2005.26.10.1560)
16. Ndlovu, T.; Arotiba, O. A.; Krause, R. W.; Mamba, B. B. *Int. J. Electrochem. Sci.* **2010**, *5*, 1179–1186.
17. Li, J.; Kuang, D.; Feng, Y.; Zhang, F.; Liu, M. *Microchim. Acta* **2011**, *172*, 379–386.
DOI: [10.1007/s00604-010-0512-0](https://doi.org/10.1007/s00604-010-0512-0)
18. Ntsendwana, B.; Mamba, B.B.; Sampath, S.; Arotiba, O.A. *Int. J. Electrochem. Sci.* **2012**, *7*, 3501–3512.
19. Cai, Y. Y.; Li, H.; Du, B.; Yang, M. H.; Li, Y.; Wu, D.; Zhao, Y. F.; Dai, Y. X.; Wei, Q. *Biomaterials* **2011**, *32*, 2117–2123.
DOI: [10.1016/j.biomaterials.2010.11.058](https://doi.org/10.1016/j.biomaterials.2010.11.058)
20. Lu, C. H.; Yang, H. H.; Zhu, C. L.; Chen, X.; Chen, G. N. *Angew Chem* **2009**, *121*, 4879–4881.
DOI: [10.1002/anie.200901479](https://doi.org/10.1002/anie.200901479)
21. Ao, Z. M.; Peeters, F. M. *J Phys Chem C* **2010**, *114*, 14503–14509.
DOI: [10.1021/jp103835k](https://doi.org/10.1021/jp103835k)
22. Wang, G.; Yang, J.; Park, J.; Gou, X.; Wang, B.; Liu, H.; Yao, J. *J. Phys. Chem. C* **2008**, *112*, 8192–8195.
DOI: [10.1021/jp710931h](https://doi.org/10.1021/jp710931h)
23. Srivastava, R. K.; Srivastava, S.; Narayanan, T. N.; Mahlotra, B. D.; Vajtai, R.; Ajayan, P. M.; Srivastava, A. *ACS Nano* **2012**, *6*, 168–175.
DOI: [10.1021/nm203210s](https://doi.org/10.1021/nm203210s)
24. Baruah, U.; Chowdhury, D. *Nanotechnology* **2016**, *27*, 145501.
DOI: [10.1088/0957-4484/27/14/145501](https://doi.org/10.1088/0957-4484/27/14/145501)
25. Zhu, S.; Zhang, J.; Tang, S.; Qiao, C.; Wang, L.; Wang, H.; Liu, X.; Li, B.; Li, Y.; Yu, W.; Wang, X.; Sun, H.; Yang, B. *Adv. Funct. Mater.* **2012**, *22*, 4732–4740.
DOI: [10.1002/adfm.201201499](https://doi.org/10.1002/adfm.201201499)
26. Baruah, U.; Deka, M. J.; Chowdhury, D. *RSC Adv.* **2014**, *4*, 36917–36922.
DOI: [10.1039/C4RA04734F](https://doi.org/10.1039/C4RA04734F)
27. Baruah, U.; Chowdhury, D. *RSC Adv.* **2016**, *6*, 67102–67112.
DOI: [10.1039/C6RA12686C](https://doi.org/10.1039/C6RA12686C)
28. Liang, H.; Raitano, J. M.; Zhang, L.; Chan, S. W. *Chem. Commun.* **2009**, *48*, 7569–7571.
DOI: [10.1039/B914447A](https://doi.org/10.1039/B914447A)
29. Zhang, Y.; Liu, Y.; Ji, X.; Banks, C. E.; Zhang, W. *J. Mater. Chem.* **2011**, *21*, 14428–14431.
DOI: [10.1039/C1JM12544C](https://doi.org/10.1039/C1JM12544C)
30. Thiago, C.; da Silva, P.; Veregue, F. R.; Aguiar, L. W.; Meneguim, J. G.; Moises, M. P.; Fa'varo, S. L.; Radovanovic, E.; Girotto, E. M.; Rinaldi, A. W. *New J. Chem.* **2016**, *40*, 8872–8877.
DOI: [10.1039/C6NJ00936K](https://doi.org/10.1039/C6NJ00936K)
31. Pogacean, F.; Biris, A. R.; Socaci, C.; Coros, M.; Magerusan, L.; Rosu, M.-C.; Lazar, M. D.; Borodi, G.; Pruneanu, S. *Nanotechnology* **2016**, *27*, 484001.
DOI: [10.1088/0957-4484/27/48/484001](https://doi.org/10.1088/0957-4484/27/48/484001)
32. Deka, M. J.; Chowdhury, D. *J. Phys. Chem. C* **2016**, *120*, 4121–4129.
DOI: [10.1021/acs.jpcc.5b12403](https://doi.org/10.1021/acs.jpcc.5b12403)
33. Zheng, Z.; Du, Y.; Wang, Z.; Feng, Q.; Wang, C. *Analyst* **2013**, *138*, 693–701.
DOI: [10.1039/c2an36569c](https://doi.org/10.1039/c2an36569c)
34. Yang, Y.-Z.; Tang, Q.; Gong, C.-B.; Ma, X.-B.; Peng, J.-D.; Lam, M. H. *New J. Chem.* **2014**, *38*, 1780–1788.
DOI: [10.1039/C3NJ01598J](https://doi.org/10.1039/C3NJ01598J)